Available online at www.sciencedirect.com

ScienceDirect

IFAC Papers Online CONFERENCE PAPER ARCHIVE

IFAC PapersOnLine 51-29 (2018) 311–316

Trajectory tracking for an articulated intervention AUV using a super-twisting algorithm in 6 DOF ⋆

I.-L. G. Borlaug * **K.Y. Pettersen** * **J. T. Gravdahl** **

* *Centre for Autonomous Marine Operations and Systems, Department of Engineering Cybernetics, NTNU, Norwegian University of Science and Technology, Trondheim, Norway (e-mail: Ida.Louise.Borlaug@ntnu.no, Kristin.Y.Pettersen@ntnu.no).*

** *Department of Engineering Cybernetics, NTNU, Norwegian University of Science and Technology, Trondheim, Norway (e-mail: Tommy.Gravdahl@ntnu.no).*

Abstract: The articulated intervention autonomous underwater vehicle (AIAUV) is a slender, multi-articulated, underwater robot that is equipped with thrusters, i.e. an underwater swimming manipulator (USM). For the AIAUV to be able to move in confined spaces and perform intervention tasks, it is essential to achieve good station-keeping and trajectory tracking performance for the AIAUV by using the thrusters and by using the joints to attain the desired position and orientation of the vehicle. In this paper, we propose a sliding mode control (SMC) law, specifically the super-twisting algorithm with adaptive gains, for the trajectory tracking of the joints angles and position and orientation of the base of the AIAUV, and we consider this tracking problem of the AIAUV in 6 DOF. A higher-order sliding mode observer is proposed for state estimation. Furthermore, we show the ultimate boundedness of the tracking errors, and we demonstrate the applicability of the proposed control law with simulations.

© 2018, IFAC (International Federation of Automatic Control) Hosting by Elsevier Ltd. All rights reserved.

Keywords: Underwater Swimming Manipulator, Super-Twisting, Siding Mode Control, Sliding Mode Observer, Autonomous Underwater Vehicle.

1. INTRODUCTION

An articulated intervention autonomous underwater vehicle (AIAUV) is an underwater swimming manipulator (USM). It has the slender, multi-articulated body of the underwater snake robot (USR), which gives the AIAUV phenomenal accessibility and flexibility, but in addition, it has multiple thrusters. The thrusters make it possible for the AIAUV to move forward without using a undulating gait pattern and give it the capability to hover. This is especially important in narrow and confined spaces, for station-keeping and trajectory tracking. These capabilities enables the AIAUV to operate as a floating base manipulator. Moreover, the AIAUV has adopted the high-kinematic redundancy of the USR and the fully energy-efficient hydrodynamic properties and tether-less operation of the autonomous underwater vehicle (AUV). Compared to standard survey AUVs, the AIAUV has the advantage that it has full actuation and it can perform intervention tasks. Since it can use its slender body to access narrow spaces, use its thrusters to keep itself stationary and then use its joints to perform intervention tasks, it can exploit the full potential of the inherent kinematic redundancy. This has been addressed in detail in (Sverdrup-Thygeson et al., 2016a), (Sverdrup-Thygeson et al., 2016b).

⋆ This research was funded by the Research Council of Norway through the Centres of Excellence funding scheme, project No. 223254 NTNU AMOS.

The AIAUV can use its slender, multi-articulated body and thrusters to move to an area of interest. It can then use its thrusters to position its base at the initial base location, and then use its joints to get the end-effector, which is positioned at the head of the AIAUV, to the desired position. It can then start to perform an intervention task. When the AIAUV performs a manipulator task, the desired velocities of the end-effector can be used to determine the overall motion of the AIAUV and the joint angles velocities. This can be done by using inverse kinematics, as done in (Sverdrup-Thygeson et al., 2017b). The outputs of this procedure are time-varying velocity references for the base and the joints, and we need a suitable tracking controller to follow these references. The design of this trajectory tracking controller for the AIAUV is one of the objectives of this paper. The performance of the tracking controller is decisive for the accuracy of the end-effector motion.

The controller design for underwater robots (URs) such as the AIAUV and remotely operated vehicles (ROVs) is a complex problem, (Antonelli, 2014). URs are often subject to hydrodynamic and hydrostatic parameter uncertainties, uncertain thruster characteristics, unknown disturbances, and unmodeled dynamic effects, e.g., thruster dynamics and coupling forces caused by joint motion. For the AIAUV the joint motion of the joints is more significant for the overall motion of the AIAUV, than for ROVs, because it has no separate vehicle base and a low mass compared

2405-8963 © 2018, IFAC (International Federation of Automatic Control) Hosting by Elsevier Ltd. All rights reserved.
Peer review under responsibility of International Federation of Automatic Control.
10.1016/j.ifacol.2018.09.506

to an ROV. This increases the complexity of the motion for the AIAUV, and therefore makes the control problem even more complex than for ROVs.

Sliding mode control (SMC) is a robust and versatile non-linear control approach that is particularly well suited for situations where unknown non-linearities affect the system, as in the case of AIAUVs. In recent years, several results have been reported on the use of SMC for many complex dynamical systems. For underwater vehicles, in general, some relevant contributions are the following: in (Antonelli and Chiaverini, 1998) an SMC approach for the regulation problem of an underwater vehicle-manipulator system is developed. This control law is inspired by Fjellstad and Fossen (1994), and it avoids the inversion of the system Jacobian, and is therefore singularity free. In (Fossen, 1991) and (Fossen and Sagatun, 1991), an SMC is used to cope with input uncertainty, due to partly known non-linear thruster characteristics. In (Soylu et al., 2008), a chattering-free SMC is proposed for trajectory control. The chattering-free approach is developed by combining the SMC with adaptive PID controller gains and having an adaptive update of the upper bound on the disturbance and parameter uncertainties. In (Dannigan and Russell, 1998), SMC is used to deal with coupling effects between a manipulator and an underwater vehicle. By combining a virtual velocity control and SMC, a hybrid control strategy is developed in (Zhu and Sun, 2013), for trajectory tracking of an unmanned underwater vehicle. In (Xu et al., 2015) the trajectory tracking problem of an under-actuated unmanned underwater vehicle is studied by combining backstepping and SMC. An attitude controller for an AUV is designed in (Cui et al., 2016), by using a sliding-mode based adaptive controller. In (Liu et al., 2017), the trajectory-tracking problem for an underwater vehicle subject to unknown system uncertainties and time-varying external disturbances is considered, and solved by using a non-linear disturbance observer-based backstepping finite-time SMC scheme. In (Rezapour et al., 2014) SMC is applied to land-based snake robots, to achieve robust tracking of a desired gait pattern and under-actuated straight-line path following.

In recent years, there has been a further development of SMC into higher-order SMC schemes, which removes the chattering problem. The super-twisting algorithm (STA) with adaptive gains, proposed by Shtessel et al. (2010) is the most powerful second-order continuous sliding mode control algorithm, as it attenuates chattering and no conservative upper bound has to be considered, to maintain sliding, because of the adaptive gains. Motivated by this, (Borlaug et al., 2018) applied the STA together with a higher-order sliding mode observer, (Kumari et al., 2016), to an USM. The tracking problem of the centre of mass of the USM was considered. The results showed that the proposed control method had excellent tracking capabilities. It gave position errors in the power of 10^{-4}m and gave a smooth control input. It was also shown that the STA with adaptive gains gave better tracking capabilities than a regular PD-controller. However, the tracking control problem was restricted to considering the position of the USM in 2 DOF and the movement of the joints were looked at as a disturbance. In this paper we extend these results by considering the vehicle in 6 DOF using an AIAUV model inspired by the 6 DOF underwater vehicle in (Antonelli, 2014) and (From et al., 2014). Specifically, we propose a super-twisting algorithm with adaptive gains for trajectory tracking control of both the position and orientation of the base in 3D, and also for the trajectory tracking of the joint angles. We also show how the 6 DOF system can be formulated such that the stability analysis done for the tracking problem in (Borlaug et al., 2018), holds for the tracking problem in 6 DOF. Finally, to illustrate our theoretical findings, we present some simulations that verify that the proposed approach is well suited for the control of AIAUVs.

The remainder of this paper is organized as follows. In Section 2 the model and the tracking control problem for the AIAUV are defined mathematically. The control law and observer design for tracking the desired trajectory are presented and analysed in Section 3. A description of the simulation model implemented for this paper and the simulation results is given in Section 4. The conclusions and suggestions for future work are given in Section 5.

2. MODELLING AND PROBLEM STATEMENT

In this section, we provide the model and the mathematical definition of the tracking control problem for the AIAUV. The AIAUV consists of n links connected by $n-1$ motorized joints. Each joint is treated as a one-dimensional Euclidean joint. To resemble the convention used in the robotics community, the first link is referred to as the base of the manipulator. The base link is link 1, and the front link, where the end-effector is positioned, is link n. The joints are numbered from $i=1$ to $n-1$, such that link i and link $i+1$ are connected by joint i. Furthermore, the AIAUV is equipped with m thrusters, including one or more thrusters acting along the body of the AIAUV to provide forward thrust, and tunnel thrusters acting through the links to provide station-keeping capability. For control purposes, the AIAUV is considered as a floating base manipulator operating in an underwater environment, subject to added mass forces, dissipative drag forces, and gravity and buoyancy forces. This allows us to model the AIAUV as an underwater vehicle-manipulator system (UVMS), with dynamic equations given in matrix form by Antonelli (2014), From et al. (2014)

$$M(q)\dot{\zeta} + C(q,\zeta)\zeta + D(q,\zeta)\zeta + g(q,\eta_2) = \tau(q) \quad (1)$$

where $q \in \mathbb{R}^{(n-1)}$ is the vector representing the joint angles, $M(q)$ is the inertia matrix including added mass terms, $C(q,\zeta)$ is the Coriolis-centripetal matrix, $D(q,\zeta)$ is the damping matrix, and $g(q,\xi)$ is the matrix of gravitational and buoyancy forces. The control input is given by the generalized forces $\tau(q)$:

$$\tau(q) = \begin{bmatrix} T(q) & 0_{6\times(n-1)} \\ 0_{(n-1)\times(6m+n-1)} & I_{(n-1)\times(n-1)} \end{bmatrix} \begin{bmatrix} \tau_{thr} \\ \tau_q \end{bmatrix} \quad (2)$$

where $T(q) \in \mathbb{R}^{n\times m}$ is the thruster configuration matrix, $\tau_{thr} \in \mathbb{R}^m$ is the vector of thruster forces, and $\tau_q \in \mathbb{R}^{(n-1)}$ represents the joint torques. To implement the control input $\tau(q)$, a thruster allocation scheme as proposed in (Sverdrup-Thygeson et al., 2017a) can be implemented to distribute the desired control inputs onto the m thrusters. The vector of body-fixed velocities, ζ, is defined by

$$\zeta = \begin{bmatrix} v^T & \omega^T & \dot{q}^T \end{bmatrix}^T \in \mathbb{R}^{6+(n-1)} \quad (3)$$

where v and ω are the body-fixed linear and angular velocities of the base of the AIAUV, and $\dot{q}$ is the vector of joint angles velocities. The complete state vector specifying the position, orientation, and shape of the AIAUV, is represented by

$$\xi = \begin{bmatrix} \eta_1^T & \eta_2^T & q^T \end{bmatrix}^T, \quad \in \mathbb{R}^{6+(n-1)} \tag{4}$$

where $\eta_1 = [x \ y \ z]^T \in \mathbb{R}^3$ is the position of the base, and $\eta_2 = [\phi \ \theta \ \psi]^T \in \mathbb{R}^3$ are the Euler angles describing the orientation of the base in the inertial frame. To complete the dynamic model we can write the relationship between the body-fixed velocities and the complete state vector as

$$\dot{\xi} = J(\eta_2)\zeta = \begin{bmatrix} R_B^I & 0_{3\times3} & 0_{3\times(n-1)} \\ 0_{3\times3} & J_{k,o}^{-1} & 0_{3\times(n-1)} \\ 0_{(n-1)\times3} & 0_{(n-1)\times3} & I_{(n-1)\times(n-1)} \end{bmatrix} \zeta \tag{5}$$

where R_I^B is the rotation matrix expressing the transformation from the inertial frame to the body-fixed frame and $J_{k,o}$ is the Jacobian matrix.

Remark 1. When using the Euler angles (xyz-convention), the Jacobian matrix is singular for $\theta = \pm\pi/2$. This could have been avoided by using quaternions, but for the state observer that we suggest in this paper, Euler angles have to be used since it does not work with a different number of states in position versus velocity. Including a state observer for quaternions is a topic for future work.

The desired velocities, are given by

$$\zeta_d = \begin{bmatrix} v_d^T & \omega_d^T & \dot{q}_d^T \end{bmatrix}^T, \tag{6}$$

in the body-fixed frame. The desired velocities, ζ_d, are typically given by the inverse kinematics as described in (Sverdrup-Thygeson et al., 2017b). The desired trajectory, $\begin{bmatrix} \eta_{1,d}^T & \eta_{2,d}^T & q_d^T \end{bmatrix}^T$ can then be reconstructed from the desired velocity, using for instance a CLIK algorithm (Siciliano and Khatib, 2008, Ch. 11). The vector of tracking errors is then defined as

$$\tilde{\xi} = \begin{bmatrix} \tilde{\eta}_1 \\ \tilde{\eta}_2 \\ \tilde{q} \end{bmatrix} = \begin{bmatrix} \eta_1 - \eta_{1,d} \\ \eta_2 - \eta_{2,d} \\ q - q_d \end{bmatrix}. \tag{7}$$

The goal of the tracking problem is, to make the error vector, $\tilde{\xi}$ converge to zero. The tracking control objective is therefore to make $(\tilde{\xi}, \tilde{\zeta}) = (0, 0)$ an asymptotically stable equilibrium point of (1) and (5), which will ensure that the tracking errors will converge to zero.

3. SLIDING MODE CONTROL

In this section, we propose a tracking control law for the AIAUV based on the theory of sliding mode control. Using Lyapunov theory , we show that $(\tilde{\xi}, \tilde{\zeta}) = (0, 0)$ is an asymptotically stable equilibrium point of (1) and (5) with the proposed control law.

3.1 State observer

As velocity measurements are not available, a state observer will be developed in this subsection. We want to use the sliding mode observer presented in (Kumari et al., 2016) because the third-order state observer has been proven finite time stable in (Moreno, 2012). In order to use this observer, we introduce a change of variables.

Change of variables Define $x_1 = \xi$ and $x_2 = J(\eta_2)\zeta$, the dynamics can then (with a slight abuse of notation) be written as

$$\begin{aligned} \dot{x}_1 &= x_2 \\ \dot{x}_2 &= \frac{d}{dt}(J(\eta_2))\zeta + J(\eta_2)\dot{\zeta} \end{aligned} \tag{8}$$

where

$$\begin{aligned} \dot{\zeta} &= M(q)^{-1}(-C(q,\zeta)\zeta - D(q,\zeta)\zeta - g(q,\eta_2) + \tau(q)) \\ &= M(q)^{-1}(-f(q,\zeta,\eta_2) + \tau(q)) \end{aligned} \tag{9}$$

and $f(q,\zeta,\eta_2) = C(q,\zeta)\zeta + D(q,\zeta)\zeta + g(q,\eta_2)$. Since $\frac{d}{dt}(J(\eta_2))$ is well defined and small, we will look at $\frac{d}{dt}(J(\eta_2))\zeta$ as a small bounded disturbance called $d(t)$.

State observer Now that we have introduced the change of variables, the state observer can be introduced. By designing the observer structure as in (Kumari et al., 2016), the state observer is chosen as

$$\begin{aligned} \dot{\hat{x}}_1 &= \hat{x}_2 + z_1 \\ \dot{\hat{x}}_2 &= \hat{x}_3 + z_2 + M(q)^{-1}J(\eta_2)\tau(q) \\ \dot{\hat{x}}_3 &= z_3 \end{aligned} \tag{10}$$

where

$$\begin{aligned} z_1 &= k_1|e_1|^{2/3}\operatorname{sgn}(e_1) \\ z_2 &= k_2|e_1|^{1/3}\operatorname{sgn}(e_1) \\ z_3 &= k_3\operatorname{sgn}(e_1) \end{aligned} \tag{11}$$

and $k_1 \in \mathbb{R}^{6+(n-1)}$, $k_2 \in \mathbb{R}^{6+(n-1)}$ and $k_3 \in \mathbb{R}^{6+(n-1)}3$ are gains to be chosen according to (Levant, 1998) and (Levant, 2003), where $e_1 = x_1 - \hat{x}_1 \in \mathbb{R}^{6+(n-1)}$. One choice of parameters that meets the requirements in (Levant, 1998) and (Levant, 2003), is according to (Chalanga et al., 2016), $k_1 = 6L^{1/3}$, $k_2 = 11L^{1/2}$ and $k_3 = 6L$, where $L \in \mathbb{R}^{6+(n-1)}$ is a sufficiently large constant. By defining $e_2 = x_2 - \hat{x}_2$ and $e_3 = -\hat{x}_3 + F(p,\zeta,\eta_2)$ where $F(p,\zeta,\eta_2) = d(t) - M(q)^{-1}J(\eta_2)f(q,\zeta,\eta_2)$, the error dynamics of the state observer can be written as

$$\begin{aligned} \dot{e}_1 &= -k_1|e_1|^{2/3}\operatorname{sgn}(e_1) + e_2 \\ \dot{e}_2 &= -k_2|e_1|^{1/3}\operatorname{sgn}(e_1) + e_3 \\ \dot{e}_3 &= -k_3\operatorname{sgn}(e_1) + \dot{F}(p,\zeta,\eta_2) \end{aligned} \tag{12}$$

If $|\dot{F}(p,\zeta,\eta_2)| < \Delta$ then the state observer errors goes to zero in finite time, (Moreno, 2012). Since $F(p,\zeta,\eta_2)$ is a combination of $\frac{d}{dt}(J(\eta_2))\zeta$, $C(q,\zeta)\zeta$, $D(q,\zeta)\zeta$ and $g(q,\eta_2)$, and since the AIAUV is a mechanical system these matrices will not change infinitely fast. It is therefore a valid assumption to assume that $\dot{F}(p,\zeta,\eta_2)$ is bounded.

3.2 Control input

In this section we will design a control law based on the super-twisting algorithm, which we in the next section will show achieves the tracking control objective.

Sliding surface To use a sliding mode control approach, we must first design a sliding surface. It should be designed such that when the sliding variable σ goes to zero, the state variables asymptotically converge to zero and such that the control input $\tau(q)$ appears in the first derivative of σ. The sliding surface is chosen as

$$\sigma = \tilde{x}_1 + \tilde{x}_2, \quad \in \mathbb{R}^{6+(n-1)} \tag{13}$$

where $\tilde{x}_1 = x_1 - x_{1,d} = \tilde{\xi}$ and $\tilde{x}_2 = x_2 - x_{2,d} = J(\eta_2)\zeta - J(\eta_{2,d})\zeta_d$. If now $\sigma = 0$, we will have $\tilde{x}_1 + \tilde{x}_2 = 0$. Since $\tilde{x}_2 = x_2 - x_{2,d} = \dot{x}_1 - \dot{x}_{1,d} = \dot{\tilde{x}}_1$, we can write this as

$$\dot{\tilde{x}}_1 = -\tilde{x}_1 \tag{14}$$

which will assure that $\tilde{x}_1$ asymptotically converges to zero. Now since $\tilde{x}_1 = \tilde{\xi}$, the state variables $\tilde{\xi}$ will also asymptotically converge to zero if $\sigma = 0$.

Since the velocity measurement is not available, the observed state values are used, and we can therefore write the sliding surface with the observed values as

$$\hat{\sigma} = \hat{\tilde{x}}_1 + \hat{\tilde{x}}_2, \quad \in \mathbb{R}^{6+(n-1)} \tag{15}$$

where $\hat{\tilde{x}}_1 = \hat{x}_1 - x_{1,d}$ and $\hat{\tilde{x}}_2 = \hat{x}_2 - x_{2,d}$. Since the state observer errors in (12) go to zero in finite time, $\hat{\sigma} = \sigma$ after some finite time. Thus, if $\hat{\sigma}$ goes to zero, the tracking objective will be satisfied.

Super-twisting algorithm In this section the equations describing the STA with adaptive gains are given in detail. The STA with adaptive gains proposed in (Shtessel et al., 2010) can be written by the update law

$$\begin{aligned} u_{\text{STA}} &= -\alpha|\sigma|^{1/2}\operatorname{sgn}(\sigma) + v, \quad \in \mathbb{R}^{6+(n-1)} \\ \dot{v} &= -\beta\operatorname{sgn}(\sigma) \end{aligned} \tag{16}$$

where the adaptive gains are defined as

$$\dot{\alpha} = \begin{cases} \omega_1\sqrt{\dfrac{\gamma_1}{2}}, & \text{if } \sigma \neq 0 \\ 0, & \text{if } \sigma = 0 \end{cases} \tag{17}$$

and

$$\beta = 2\varepsilon\alpha + \lambda + 4\varepsilon^2 \tag{18}$$

where $\varepsilon \in \mathbb{R}^{6+(n-1)}$, $\lambda \in \mathbb{R}^{6+(n-1)}$, $\gamma_1 \in \mathbb{R}^{6+(n-1)}$ and $\omega_1 \in \mathbb{R}^{6+(n-1)}$ are positive constants and σ is the sliding surface. For implementation purposes, a small boundary is put on the sliding surface so the adaptive gains can be expressed as

$$\begin{aligned} \dot{\alpha} &= \begin{cases} \omega_1\sqrt{\dfrac{\gamma_1}{2}}, & \text{if } |\sigma| > \alpha_m \\ 0, & \text{if } |\sigma| \leq \alpha_m \end{cases} \\ \beta &= 2\varepsilon\alpha_x + \lambda + 4\varepsilon^2 \end{aligned} \tag{19}$$

where the design parameter α_m is a small positive constant chosen empirically. The STA with adaptive gains makes σ and $\dot{\sigma}$ go to zero in finite time, (Shtessel et al., 2010).

Control input By designing the control input $\tau(q)$ such that $\dot{\hat{\sigma}} = u_{\text{STA}}$, we thus achieve that $\hat{\sigma}$, $\dot{\hat{\sigma}}$ reach zero in finite time since the STA is finite time stable. Taking the time derivative of (15) and substituting $\dot{\hat{x}}_1$ and $\dot{\hat{x}}_2$, defined in (10), we find that

$$\begin{aligned} \dot{\hat{\sigma}} =& \dot{\hat{\tilde{x}}}_1 + \dot{\hat{\tilde{x}}}_2 = \dot{\hat{x}}_1 - \dot{x}_{1,d} + \dot{\hat{x}}_2 - \dot{x}_{2,d} \\ =& \hat{x}_2 + z_1 - \dot{x}_{1,d} + \hat{x}_3 + z_2 + \\ & M(q)^{-1}J(\eta_2)\tau(q) - \dot{x}_{2,d} \end{aligned} \tag{20}$$

By choosing $\tau(q)$ to be

$$\begin{aligned} \tau(q) =& J(\eta_2)^{-1}M(q)(-\hat{x}_2 - z_1 + \dot{x}_{1,d} - \\ & \hat{x}_3 - z_2 + \dot{x}_{2,d} + u_{\text{STA}}) \end{aligned} \tag{21}$$

we obtain

$$\dot{\hat{\sigma}} = u_{\text{STA}}. \tag{22}$$

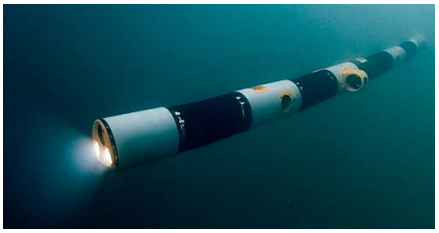

Fig. 1. The Eelume vehicle (Courtesy: Eelume)

3.3 Stability

In this section we perform a stability analysis of the closed-loop system, and it is shown that the tracking error converges asymptotically to zero.

Overall closed-loop dynamics We consider the the closed-loop system (1), (5), (21). By using the fact that $\hat{x}_1 = x_1 - e_1$ and that $\hat{x}_2 = x_2 - e_2$, from Section 3.1.2, (15) can be written as

$$\begin{aligned} \hat{\sigma} &= x_1 - e_1 - x_{1,d} + x_2 - e_2 - x_{2,d} \\ &= \tilde{\xi} - e_1 + \dot{\tilde{\xi}} - e_2. \end{aligned} \tag{23}$$

By rearranging, we get that the tracking error dynamics is

$$\dot{\tilde{\xi}} = -\tilde{\xi} + \hat{\sigma} + e_1 + e_2. \tag{24}$$

Furthermore, the velocity tracking error $\tilde{\zeta}$ is represented by the sliding variable $\hat{\sigma}$, cf. (15) and (8). The overall closed-loop dynamics with $\tau(q)$ given by (21) is thus given by $\dot{\hat{\sigma}}$ given in (22), $\dot{\tilde{\xi}}$ given in (24) and the state observer error given in (12). The closed-loop dynamics is thus:

$$\begin{aligned} \sum_1 & \begin{cases} \dot{\tilde{\xi}} = -\tilde{\xi} + \hat{\sigma} + e_1 + e_2 \\ \dot{\hat{\sigma}} = -\alpha|\hat{\sigma}|^{1/2}\operatorname{sgn}(\hat{\sigma}) + v \\ \dot{v} = -\beta\operatorname{sgn}(\hat{\sigma}) \end{cases} \\ \sum_2 & \begin{cases} \dot{e}_1 = -k_1|e_1|^{2/3}\operatorname{sgn}(e_1) + e_2 \\ \dot{e}_2 = -k_2|e_1|^{1/3}\operatorname{sgn}(e_1) + e_3 \\ \dot{e}_3 = -k_3\operatorname{sgn}(e_1) + \dot{F}(p, \zeta, \eta_2) \end{cases} \end{aligned} \tag{25}$$

We have thus obtained the closed-loop system in the desired form, such that from (Borlaug et al., 2018, Theorem 1) we have that the system is uniformly globally asymptotically stable.

4. SIMULATION RESULTS

4.1 Implementation

The complete model and controller is implemented in MATLAB Simulink. The AIAUV implemented is based on the Eelume robot, Fig. 1. It has $n = 9$ links and $m = 7$ thrusters. In Tab. 1 the properties of each link can be found. In the thrusters column, "2: Z, Y" means that the links has 2 thrusters, one working in the z-direction and one working in the y-direction. Since the robot has $n = 9$ links, it has $n - 1 = 8$ joints. All the joints where implemented as revolute. The joint properties can be found in Tab. 2. In the simulation we use a inverse kinematic controller to give us the reference that we want the AIAUV to follow, as proposed in (Sverdrup-Thygeson et al., 2017a). The thruster allocation matrix is also implemented as in (Sverdrup-Thygeson et al., 2017a).

Table 1. Eelume link properties

Link nr.	Length [m]	Volume [m^3]	Thrusters
1	0.62	0.143	0
2, 4, 6, 8	0.104	0.06	0
3	0.584	0.127	2: Z, Y
5	0.726	0.098	3: X, X, Z
7	0.584	0.127	2: Y, Z
9	0.37	0.078	0

Table 2. Eelume joint properties

Joint nr.	Direction
1, 3, 5, 7	Z
2, 4, 6, 8	Y

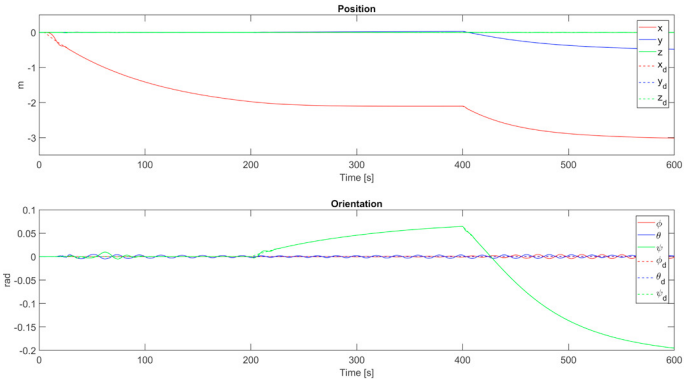

Fig. 2. Position and orientation of the base

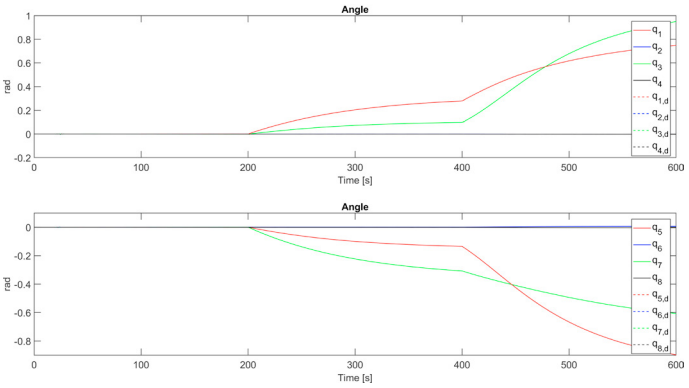

Fig. 3. Joint angles

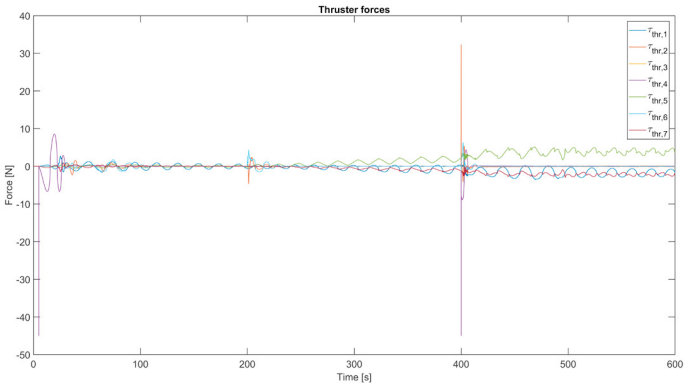

Fig. 4. Thruster forces

4.2 Simulations

The simulation done is set-point regulation for the end-effector of the AIAUV. Inverse kinematics is then used to create a reference trajectory for the base and joints to follow. Note that since inverse kinematic is used to create the references the initial errors of the base are zero, since the inverse kinematic uses the initial position of the base to create the references. The initial errors of the end-effector are on the other hand not equal to zero. As described in Section 3.1.2 the gain parameter L chosen needs to be sufficiently large, and for the simulations, L was tuned manually to obtain good performance. Since the STA has an adaptive gain α, the choice of parameters is not that important. The choice of gains can impact how fast the adaptive gain reaches its optimal value, but it will always reach that value. The gains for the STA were therefore chosen by tuning them manually. Specifically, the gains in the super-twisting algorithm with adaptive gains were set to $\varepsilon = [0.0001e_{14}]^T$, $\lambda = [0.1e_6 \quad 5e_8]^T$, $\gamma_1 = [e_{14}]^T$, $\omega_1 = [8e_{14}]^T$, $\alpha_m = [0.005e_{14}]^T$, and the observer gain was set to $L = [6e_{14}]^T$, where e_i is a $1 \times i$ vector with ones. For the simulations, a fixed-step solver, with fixed step size 10^{-5} was used. In Tab. 3, the maximum position error after settling is presented. In Fig. 2, the simulation results for the position and orientation of the base are presented. In Fig. 3, the simulation results for the joint angles are presented, and in Fig. 4 the thruster forces applied are presented.

4.3 Discussion

We can see from Fig. 2 and Fig. 3 that the AIAUV follows the given position, orientation and joints trajectories very well. This can also be seen from Tab. 3. This confirms the theoretical results of Section 4. From Fig. 4 we can see that the thruster forces used is below $50N$ which is the limit of the thrusters on the actual Eelume robot. That means that the forces used to control the AIAUV is indeed applicable.

5. CONCLUSIONS AND FUTURE WORK

In this paper, we have discussed the use of the AIAUV as a floating base manipulator, for which the trajectory tracking performance is important, and how the complexity of motion control is larger for AIAUVs than for ROVs. We have proposed a second-order sliding mode control law for trajectory tracking and used a sliding mode observer for the case when velocity measurements are not available.

Table 3. Absolute maximum value for errors

	Errors	
	Before settling	After settling
x	0.1014m	$4.2240 \cdot 10^{-4}$m
y	0.0078m	$3.3649 \cdot 10^{-4}$m
z	0.0116m	0.0023m
ϕ	0.0048	0.0043
θ	0.0051	0.0023
ψ	0.0100	$2.5682 \cdot 10^{-7}$
q_1	0.0018	$1.8732 \cdot 10^{-7}$
q_2	0.0011	$1.7646 \cdot 10^{-7}$
q_3	0.0034	$3.0269 \cdot 10^{-7}$
q_4	0.0025	$1.3706 \cdot 10^{-7}$
q_5	$8.8742 \cdot 10^{-4}$	$2.3196 \cdot 10^{-7}$
q_6	0.0022	$1.1751 \cdot 10^{-7}$
q_7	$6.5230 \cdot 10^{-4}$	$2.1077 \cdot 10^{-7}$
q_8	$4.5640 \cdot 10^{-4}$	$1.4460 \cdot 10^{-7}$

Furthermore, we have proved the asymptotic convergence of the tracking error and performed a simulation study to verify the applicability of the proposed control law in 6 DOF.

Future work includes investigating how the proposed control systems handles disturbances, and performing experiments to investigate the performance of the control algorithm in practice.

ACKNOWLEDGEMENTS

This research was funded by the Research Council of Norway through the Centres of Excellence funding scheme, project No. 223254 NTNU AMOS.

REFERENCES

Antonelli, G. and Chiaverini, S. (1998). Singularity-free regulation of underwater vehicle-manipulator systems. In *Proc. American Control Conference.*, 399–403. Philadelphia, Pennsylvania.

Antonelli, G. (2014). *Underwater Robots*, volume 96 of *Springer Tracts in Advanced Robotics*. Springer International Publishing, 3rd ed. 2014. edition.

Borlaug, I.L.G., Gravdahl, J.T., Sverdrup-Thygeson, J., Pettersen, K.Y., and Loria, A. (2018). Trajectory tracking for underwater swimming manipulator using a super twisting algorithm. *Asian Journal of Control (Accepted)*.

Chalanga, A., Kamal, S., Fridman, L.M., Bandyopadhyay, B., and Moreno, J.A. (2016). Implementation of Super-Twisting Control: Super-Twisting and Higher Order Sliding-Mode Observer-Based Approaches. *IEEE Transactions on Industrial Electronics*, 63(6), 3677–3685.

Cui, R., Zhang, X., and Cui, D. (2016). Adaptive sliding-mode attitude control for autonomous underwater vehicles with input nonlinearities. *Ocean Engineering*, 123, 4554.

Dannigan, M.W. and Russell, G.T. (1998). Evaluation and reduction of the dynamic coupling between a manipulator and an underwater vehicle. *IEEE Journal of Oceanic Engineering.*, 23(3), 260–273.

Fjellstad, O.E. and Fossen, T.I. (1994). Singularity-free tracking of unmanned underwater vehicles in 6 DOF. In *Proc. 33rd IEEE Conference on Decision and Control.*, 1128–1133. Lake Buena Vista, Florida.

Fossen, T.I. (1991). Adaptive macro-micro control of nonlinear underwater robotic systems. In *Proc. 5th International Conference on Advanced Robotics.*, 1569–1572. Pisa, Italy.

Fossen, T. and Sagatun, S. (1991). Adaptive control of nonlinear underwater robotic systems. *Modeling, Identification and Control*, 12(2), 95–105.

From, P.J., Gravdahl, J.T., and Pettersen, K.Y. (2014). *Vehicle-Manipulator Systems: Modeling for Simulation, Analysis, and Control*. Advances in Industrial Control. Springer-Verlag.

Kumari, K., Chalanga, A., and Bandyopadhyay, B. (2016). Implementation of Super-Twisting Control on Higher Order Perturbed Integrator System using Higher Order Sliding Mode Observer. In *Proc. 10th IFAC Symposium on Nonlinear Control Systems.*, volume 49, 873–878. California, USA.

Levant, A. (2003). Higher-order sliding modes, differentiation and output-feedback control. *International Journal of Control*, 76(9-10), 924–941.

Levant, A. (1998). Robust exact differentiation via sliding mode technique. *Automatica*, 34(3), 379–384.

Liu, S., Liu, Y., and Wang, N. (2017). Nonlinear disturbance observer-based backstepping finite-time sliding mode tracking control of underwater vehicles with system uncertainties and external disturbances. *Nonlinear Dynamics*, 88(1), 465–476.

Moreno, J.A. (2012). Lyapunov function for Levant's Second Order Differentiator. In *Proc. IEEE 51st IEEE Conference on Decision and Control*, 6448–6453. Maui, Hawaii, USA.

Rezapour, E., Pettersen, K.Y., Liljebäck, P., and Gravdahl, J.T. (2014). Differential geometric modelling and robust path following control of snake robots using sliding mode techniques. In *Proc. 2014 IEEE International Conference on Robotics and Automation.*, 4532–4539. Hong Kong, China.

Shtessel, Y.B., Moreno, J.A., Plestan, F., Fridman, L.M., and Poznyak, A.S. (2010). Super-twisting adaptive sliding mode control: A Lyapunov design. In *Proc. 49th IEEE Conference on Decision and Control.*, 5109–5113. Atlanta, GA, USA.

Siciliano, B. and Khatib, O. (2008). *Springer Handbook of Robotics*. Springer, Berlin.

Soylu, S., Buckham, B.J., and Podhorodeski, R.P. (2008). A chattering-free sliding-mode controller for underwater vehicles with fault-tolerant infinity-norm thrust allocation. *Ocean Engineering*, 35(16), 1647–1659.

Sverdrup-Thygeson, J., Kelasidi, E., Pettersen, K.Y., and Gravdahl, J.T. (2016a). A control framework for biologically inspired underwater swimming manipulators equipped with thrusters. In *Proc. 10th IFAC Conference on Control Applications in Marine Systems*, volume 49, 89–96. Trondheim, Norway.

Sverdrup-Thygeson, J., Kelasidi, E., Pettersen, K.Y., and Gravdahl, J.T. (2016b). The Underwater Swimming Manipulator - A Bio-Inspired AUV. In *Proc. 2016 IEEE OES Autonomous Underwater Vehicles.*, 387–395. Tokyo, Japan.

Sverdrup-Thygeson, J., Kelasidi, E., Pettersen, K.Y., and Gravdahl, J.T. (2017a). The underwater swimming manipulator - a bioinspired solution for subsea operations. *IEEE Journal of Oceanic Engineering*, PP(99), 1–16.

Sverdrup-Thygeson, J., Moe, S., Pettersen, K.Y., and Gravdahl, J.T. (2017b). Kinematic singularity avoidance for robot manipulators using set-based manipulability tasks. In *Proc. 1st IEEE Conference on Control Technology and Applications.*, 142–149. Kohala Coast, Hawaii.

Xu, J., Wang, M., and Qiao, L. (2015). Dynamical sliding mode control for the trajectory tracking of underactuated unmanned underwater vehicles. *Ocean Engineering*, 105, 54–63.

Zhu, D. and Sun, B. (2013). The bio-inspired model based hybrid sliding-mode tracking control for unmanned underwater vehicles. *Engineering Applications of Artificial Intelligence*, 25(10), 2260–2269.